Supplemental Material : Details of Simulation

Title Krill-eye : Superposition Compound Eye
for Wide-Angle Imaging via GRIN Lenses

author Shinsaku Hiura[1], Ankit Mohan and Ramesh Raskar, MIT Media Lab

Paper ID AW-19-009

This document describes the details of our simulation. We simulate the necessary optical phenomena that affect the image quality. We also show the results with an angle limiter.

1 Simulated Optical Phenomena

1.1 Misalignment Error

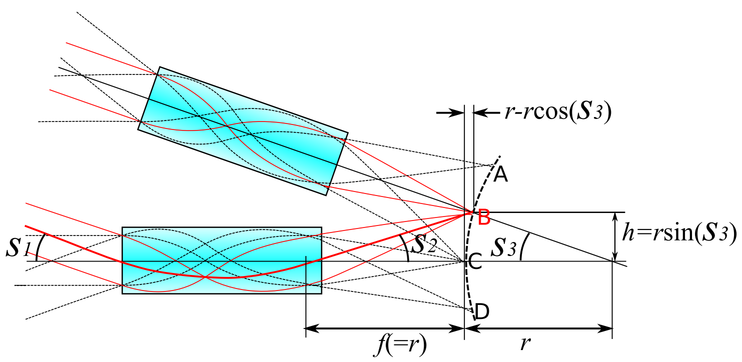

Figure 1: Misalignment error caused by the curvature of the image surface. Since the distance from the GRIN lens to the image point B is longer than the radius of the image surface, angle $S_2(= S_1)$ is smaller than S_3. The error rapidly converges to zero according to the decreasing S_3 as shown in Fgiure 5(a) in the paper.

[1]now at Osaka University

As described at Section 2.2 in the paper, the viewing angle S_1 from the bottom lens shown in Figure 1 is a little smaller than the ideal angle S_3. The angle S_2 is given by

$$S_2 = tan^{-1} \frac{r \sin(S_3)}{f + r - r \cos(S_3)} \tag{1}$$

where *superposition constraint* $r = f$ must be satisfied. Therefore we use the equation

$$S_1 = S_2 = tan^{-1} \frac{\sin(S_3)}{2 - \cos(S_3)} \tag{2}$$

for our simulation. The error $S_3 - S_1$ rapidly converges to zero according to the decreasing S_3 as shown in Fgiure 5(a) in the paper.

1.2 Vignetting of Each Ommatidium

Vignetting (illuminance distribution of the image) affects to the quality of superposed image because lower brightness at the periphery of the image circle reduces the effect of the misalignment error. The distribution of the brightness of the GRIN lens have been studied[1, 2, 3]. It is known that the off-axis irradiance from a single GRIN lens follows an ellipsoidal distribution,

$$\left(\frac{h}{h_0}\right)^2 + \left(\frac{k}{k_0}\right)^2 = 1 \tag{3}$$

where h/h_0 is the ratio of the irradiance between the center and the off-axis point at a distance from the optical axis of k. k_0 is the radius of the image circle of the lens. The maximum angle of the light θ passing through the GRIN lens is given by

$$\theta = \tan\left(\frac{k_0}{f}\right) = sin^{-1}\left(n_0 \frac{D\sqrt{A}}{2}\right) \tag{4}$$

where D is the diameter of the GRIN lens. GRIN lenses on the market have FOV between $43°$ and $72°$ with the diameter between 1.0 and 2.0. Thinner lens currently used for the scanners may have a little smaller angle. Therefore, 30° FOV we used for the simulation is not optimistic at all.

1.3 Defocus and Chromatic Aberration

The curvature of the image surface also introduces the defocus in the image. The circle of confusion at the point B in Figure 1 is given by

$$\frac{r - r\cos(S_3)}{F} = \frac{D(r - r\cos(S_3))}{f}. \tag{5}$$

Since the diameter of the GRIN lens D is much smaller than f, the effect of the defocus is always much smaller than the misalignment error.

2 Angle Limiter

Since the periphery of the image formed by each GRIN lens causes misalignment error, the field of view should be adequately limited to acquire a better image. Therefore we introduced an angle limiter to mask the certain parts of the image.

As shown in Figure 2, we use mask like vertical stripes to cover the both left and right sides of the image. The field of view is automatically tuned to six times larger than the angle between two GRIN lenses. In other words, six images are superposed at every point.

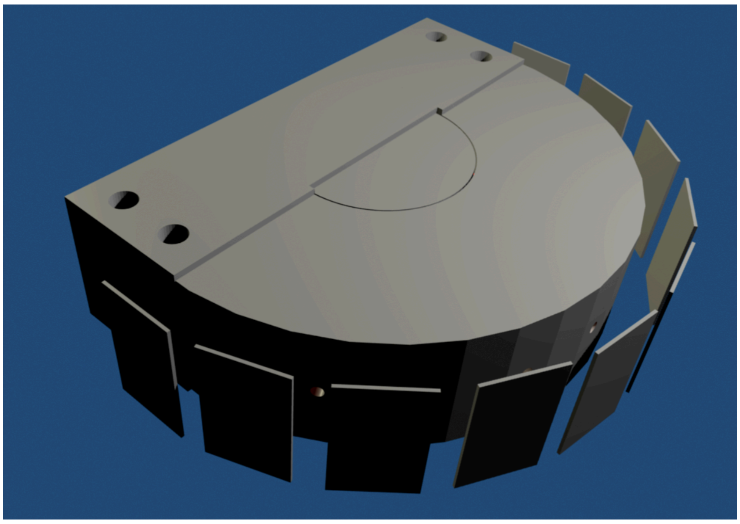

Figure 2: The schematic view of angle limiter. for 2-D (cylindrical) case, angle limiter is placed vertically to mask the portion of the image that causes superposition error.

We simulate the angle limiter with a gap whose width is the as same as the diameter of the GRIN lens as shown in Figure 3. The angle of limited field of view S_L depends on the depth of the slit, L as

$$S_L = 2\tan\left(\frac{D}{L}\right), \tag{6}$$

where D is the diameter of the GRIN lens. As described before, we set the field of view to six times the angle between two GRIN lenses, $S_L = 6 \cdot S_3$. Therefore, the depth of the gap can be calculated as

$$L = \frac{D}{\tan^{-1}(3S_3)}. \tag{7}$$

Top view of the angle limiter and a GRIN lens is also shown in Figure 3 right. The aperture of the GRIN lens is partially masked with the angle limiter, and the shape of the effective aperture is a part of a circle. The area of the effective aperture A is given

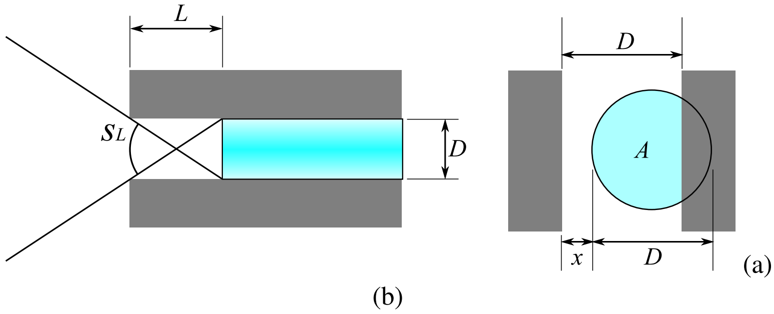

Figure 3: Parameters of the angle limiter. (a) Side view. Field of view S_L is determined by the depth of the angle limiter L. (b) Top view. The area of the effective aperture depends on the angular position of the object.

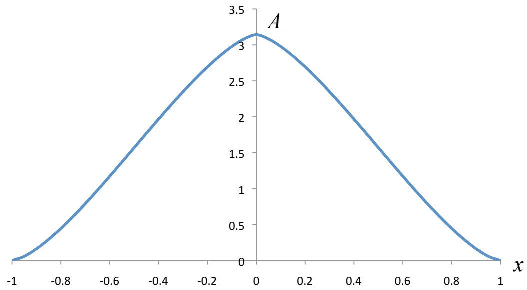

Figure 4: The distribution of the illuminance given by the angle limiter.

by

$$A = 2D^2 \int_{-1}^{1-2\frac{|x|}{D}} \sqrt{1-t^2}dt. \tag{8}$$

The distribution of light fall-off according to the angular shift is shown in Figure 4.

References

[1] C. GOMEZ-REINO, E. ACOSTA, and M. PEREZ. Limitation in the cone of light through grin lenses : Stops, pupils and vignetting. *Japanese journal of applied physics. Pt. 1, Regular papers and short notes*, 31(5):1582–1585, 19920530.

[2] K. Matsuhita and M. Toyama. Unevenness of illuminance caused by gradient-index fiber arrays. *Applied Optics*, 19:1070–1075, 1980.

[3] J. D. Rees and W. Lama. Some radiometric properties of gradient-index fiber lenses. *Applied Optics*, 19:1065–1069, 1980.